Academic Journal of Science and Technology
ISSN: 2771-3032 | Vol. 11, No. 3, 2024

Analysis and Study on Dynamic Elastic-plastic Time History of Damaged Steel Frame Structures

Donghan Li

Central South University of Forestry and Technology, China

Abstract: Combining the moment-curvature relationship of the damaged section of the component, dynamic elastoplastic time-history analysis was conducted on the damaged steel frame structure. Using general finite element analysis software, the structural response of the damaged steel frame structure under the action of multiple seismic waves was studied, analyzing the influence of variations in different structural parameters on the seismic performance of the damaged steel frame structure.

Keywords: Prefabricated PC Frame Structure; Section Steel Connection; Seismic Performance.

1. Introduction

Steel frame structures are essential components of modern construction, offering high strength-to-weight ratios and ductility vital for seismic resilience. Assessing their dynamic behavior under seismic loading is critical for ensuring structural safety in earthquake-prone areas. Elastoplastic dynamic time-history analysis provides a comprehensive method for evaluating the seismic performance of steel frame structures by considering material nonlinearities and dynamic effects.

Recent research has focused on studying the response of steel frame structures to seismic actions, particularly exploring how parameters like the number of storeys and spans affect structural behavior. Finite element analysis has emerged as a powerful tool for simulating structural responses to seismic loading, allowing for detailed investigations. OpenSees, a robust software framework, has gained prominence for conducting finite element analyses in earthquake engineering and structural dynamics. Its capabilities in modeling material behavior and simulating structural responses make it well-suited for studying the seismic performance of steel frame structures. This study aims to enhance understanding of elastoplastic dynamic time-history analysis of damaged steel frame structures under seismic actions using OpenSees software. By constructing finite element models and analyzing seismic records, the seismic performance of structures with varying parameters will be evaluated. Specifically, the influence of the number of storeys and spans on structural deformation capacity and damage accumulation will be explored.

The findings are expected to provide insights into the behavior of steel frame structures under seismic loading, aiding in the development of seismic design guidelines and retrofit strategies for improving structural resilience in earthquake-prone regions.

1.1. Selection of Earthquake Ground Motion Records

Research shows that in the statistical analysis of seismic response affecting structures, the uncertainty of earthquake ground motion often has a greater impact on the results than the uncertainty of the structure's own characteristics. Sometimes, the uncertainty of earthquake ground motion may even overshadow the uncertainty of structural characteristics.

The American ATC-63 (2008) report [1] recommends selecting 22 far-field earthquake ground motions and 28 near-field earthquake ground motions based on the following principles:

(1) Choose earthquakes with magnitudes greater than 6.5 to ensure sufficient energy to affect structures.

(2) Prioritize earthquakes of strike-slip or thrust fault types, primarily focusing on seismic characteristics in regions like California, USA.

(3) Select earthquake ground motion records from rock or hard soil sites [2] to avoid foundation damage issues caused by soft soil.

(4) Ensure that the hypocentral distance exceeds 10 kilometers to distinguish between characteristics of near-field and far-field ground motions [3, 4].

(5) Limit the number of earthquake ground motions from the same seismic event to no more than two to enhance the broad applicability of the data.

(6) Choose earthquake ground motions with peak ground acceleration (PGA) greater than 0.2g and peak ground velocity (PGV) greater than 15 centimeters per second.

(7) Ensure that the effective period of the earthquake ground motion is at least 4 seconds.

(8) Install strong motion instruments on free-field sites or ground floors of small buildings, considering the effects of structure-soil coupling on earthquake ground motions.

The analysis model site is classified as a Site Class II site, which corresponds to the S2 site classification standard of the United States Geological Survey (USGS). Following the wave selection principles of ATC-63, 14 earthquake records that meet the criteria of wave velocity range and hypocentral distance standards were selected from the PEER Strong Motion Database [64], as shown in Table 1

2. Establishment of Finite Element Model

2.1. Basic Structural Model Parameters

The basic geometric parameters of the damaged steel frame structure finite element model are as follows: floor height is 3.5m, span is 6m, site class is Class II, seismic grouping is the first group, seismic fortification intensity is 8 degrees, design basic acceleration value is 0.2g, and the steel strength grade is Q235. The first two modal periods of the structure are 0.2852s and 0.0886s respectively. The loading condition of

the damaged steel frame is shown in Figure 1.

Table 1. Ground motion recording

Name	Earthquake Time	Magnitude	Seismic Station	PGA(g)	Component
Northridge1	1994	6.7	Beverly Hills-Mulhol	0.52	NORTHR/MUL279
Imperial, Valley1	1979	6.5	Delta	0.35	IMPVALL /H-DLT352
Imperial, Valley2	1979	6.5	E1 Centro Array # 11	0.38	IMPVALL/H-E11230
Kobe, Japan1	1995	6.9	Nishi-Akashi	0.51	KOBE/NIS000
Kocaeli, Turkey1	1999	7.5	Duzce	0.36	KOCAELI/DZC270
L anders1	1992	7.3	Yermo Fire Station	0.24	LANDERS/YER270
L anders2	1992	7.3	Coolwater	0.42	L ANDERS/CLW-TR
L .oma Prieta1	1989	6.9	Capitola	0.53	L. OMAP/C AP000
L .oma Prieta2	1989	6.9	Gilroy Array #3	0.56	LOMAP/GO3000
Superstition Hills1	1987	6.5	EI Centro Imp. Co.	0.36	SUPERST/B-ICC000
Cape Mendocino	1992	7	Rio Dell Overpass	0.55	CAPEMEND/RIO360
Chi-Chi, Taiwan2	1999	7.6	TCU045	0.51	CHICHI/TCU045-N
San Fernando	1971	6.6	LA-Holly wood Stor	0.21	SRERNPEL090
Friuli, Italy	1976	6.5	Tolmezzo	0.35	FRIULI/A-TMZ000

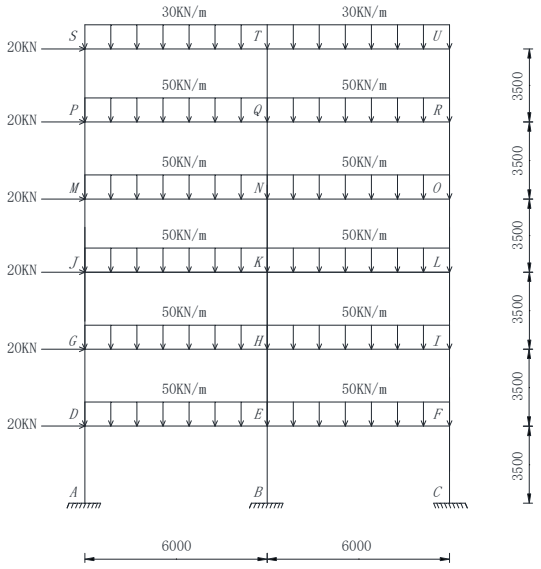

Fig 1. Structural stress diagram

2.2. Definition of Sectional Damage Index D

In classical damage mechanics, let E_0 and $\breve{E}$ represent the elastic modulus of undamaged and damaged materials, respectively. Based on the concept of effective stress, by introducing the effective elastic modulus instead of effective stress, the method for calculating the elasticity of tensile-damaged materials can be directly derived from the undamaged material model. The damage index of the damaged section during analysis is calculated using the following formula [2]:

$$D = \eta(1 - \frac{\overline{E}}{E_0}) \tag{1}$$

In the equation, η represents the damage amplification factor ($\eta = 2.7970$).

The decrease in the elastic modulus ratio is used as a measure of the degree of damage to the damaged section, ranging between 0 and 1. When the stiffness reduction ratio is 0, it indicates that the material has not been damaged; whereas when the stiffness reduction ratio is 1, it indicates that the material has been completely destroyed.

2.3. Parameters of the Damaged Section

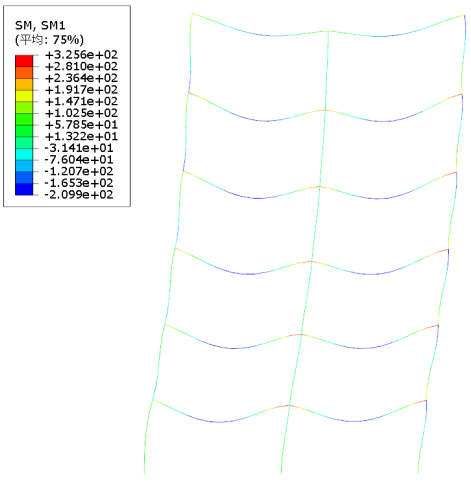

Fig 2. Basic model stress nephogram

Based on the loading conditions of the damaged steel frame structure model parameters, the stress contour map of the basic model of the damaged steel frame structure is calculated and shown in Figure 2.

Based on the stress contour map of the basic model of the damaged steel frame structure, it can be determined that the maximum moment occurs at the right end of the beam in the second span. In the calculation results, it was found that the moment values at points I, L, and O exceeded the initial yield moment. This indicates that plastic deformation zones have formed at the ends of members HI, KL, and NO. Three different damage degrees of moment-curvature relationships were obtained, and these relationships were input into the zero Length elements at the ends of members HI, KL, and NO. The sectional damage indices D at points I, L, and O were calculated as shown in Table 2.

Table 2. Basic model cross-section damage index

End Node	Sectional Damage Index D
I	0.3728
L	0.4652
O	0.3912

2.4. Steps for Establishing the Finite Element Model

First, use the model BasicBuilder command to define the number of dimensions (ndm) and the degrees of freedom (ndf) for each node. For a two-dimensional problem, each node requires three degrees of freedom: two translations in the plane and one rotation around the plane normal. Additionally, ensure that the units used throughout the program are consistent: force in Newtons (N), length in millimeters (mm), weight in tons (t), and time in seconds (s).

After defining the dimensions and degrees of freedom for each node, input the basic parameters of the frame structure: the number of floors, the number of spans, span length, first-floor height, and the height of subsequent floors. Next, input the material properties: the elastic modulus and yield strength. Finally, input the beam and column section parameters: cross-sectional area, moment of inertia, plastic modulus, section height, section width, flange plate thickness, web plate thickness, and beam/column height.

The procedure involves looping through earthquake waves, performing amplitude modulation analysis to simulate earthquakes of varying intensities. Recorders are set up to monitor floor displacement angles. For each PGA level, the analysis state and time are reset, and earthquake load patterns based on the adjusted PGA values are created and applied with uniform excitation. Solver components such as constraint handling, numberer, system, convergence test, algorithm, and integration method are set up. Nonlinear dynamic analysis is conducted using the Newmark integration method and the Newton algorithm with constitutive relation corrected. Transient analysis is performed for each PGA level to simulate seismic responses. Once completed, load patterns and recorders are removed, and the model is reset. After analysis, all recorders are removed, the model is reset, and a message "Vulnerability analysis complete" is output to signify completion of vulnerability analysis. Finally, all definitions are cleared.

3. Parameter Analysis

3.1. The Influence of Number of Floors on the Damaged Steel Frame Structure

Using the finite element design analysis software OpenSees, the basic model underwent elastoplastic dynamic time-history analysis under the action of 14 earthquake ground motions. By comparing the column top displacement time-history curves of three-story, six-story, and nine-story structures, the maximum column top displacement under different earthquake ground motions was obtained.

Table 3. The maximum top displacements for the three-story, six-story, and nine-story structures.

Floor	Name	Duration(s)	Maximum Top Displacement(mm)
3	Imperial, Valley1	99.91	69.12
6	L. oma Prieta1	39.95	348.52
9	Kobe, Japan1	40.95	1170.24

Through comparing the variations in top displacement of damaged steel frame structures with different numbers of floors during seismic events, it was observed that the maximum top displacement increased with the number of floors: 69.12 millimeters for the three-story structure during the Imperial Valley1 earthquake, 292 millimeters for the six-story structure during the Cape Mendocino earthquake, and 1170 millimeters for the nine-story structure during the Kobe Japan1 earthquake. These findings suggest that as the number of floors increases, the top displacement of structures during earthquakes also increases, indicating a significant increase in seismic sensitivity and vulnerability with additional floors under the same damage conditions.

3.2. The Influence of Structural Span Number on the Damaged Steel Frame Structure

Using the finite element design analysis software OpenSees, the basic model underwent elastoplastic dynamic time-history analysis under the action of 14 earthquake ground motions. By comparing the column top displacement time-history curves of the six-story single-span, six-story double-span, and six-story triple-span structures, the maximum column top displacement under different earthquake ground motions was obtained.

Table 4. Maximum Top Displacement for Single-Span, Double-Span, and Triple-Span Structures

Span	Name	Duration(s)	Maximum Top Displacement(mm)
1	Kocaeli, Turkey1	27.18	224.09
2	L .oma Prieta1	39.95	348.52
3	Imperial, Valley2	30.03	399.01

Comparing the top displacement variations of damaged steel frame structures with different numbers of floors during seismic events revealed significant differences. For instance, during the Imperial Valley1 earthquake, the three-story structure exhibited a maximum top displacement of 69.12 millimeters, while under the influence of the Cape Mendocino earthquake, the six-story structure experienced a maximum top displacement of 292 millimeters. However, during the Kobe Japan1 earthquake, the nine-story structure recorded a remarkable maximum top displacement of 1170 millimeters. These data underscore that as the number of floors increases, the top displacement of structures during earthquakes also increases, with a particularly notable escalation from six to nine floors. Under similar damage conditions, the seismic sensitivity and vulnerability of structures substantially increase with additional floors.

3.3. The Influence of Damage Severity on the Damaged Steel Frame Structure

Assuming three structural models have the same parameters but different loading conditions for a six-story damaged steel frame structure, we calculate the maximum damage indices D for the sections to be 0.6992 and 0.8755. We name the undamaged steel frame model with a maximum damage index D of 0 as SF0, and the damaged steel frame structures with maximum damage indices of 0.4652, 0.6992, and 0.8755 as SF1, SF2, and SF3, respectively, where SF1 represents the basic model.

Using the finite element design analysis software OpenSees, the basic model underwent elastoplastic dynamic time-history analysis under the action of 14 earthquake ground motions. By comparing the column top displacement time-history curves of the damaged steel frame structures SF1, SF2, and SF3, the maximum column top displacement under different earthquake ground motions was obtained.

Table 5. Maximum Top Displacement for SF1, SF2, and SF3

Damaged Frame	Name	Duration(s)	Maximum Top Displacement(mm)
SF1	L .oma Prieta1	39.95	348.52
SF2	L .oma Prieta1	39.95	475.20
SF3	Kocaeli, Turkey1	27.18	565.54

In the early stages of damage, the maximum top displacement of the steel frame structure does not show significant changes as the damage index increases from 0 to 0.4652. However, with the further increase in the maximum node damage index, there is a rising trend in the maximum top displacement. Specifically, as the damage index increases from 0.4652 to 0.6992, the maximum top displacement of the structure significantly increases, reaching an increment of 183 millimeters. When the damage index increases from 0.6992 to 0.8755, the increase in top displacement appears to be slower compared to the increase from 0.4652 to 0.6992. This phenomenon may be attributed to the structural components nearing or reaching their ultimate load-bearing capacity as the damage worsens. With the further increase in the damage index, the displacement increment of these components or the overall structural displacement may no longer be significant. Additionally, certain regions of the structure may have reached their deformation limits, thereby unable to produce significant deformations further.

4. Conclusion

This study investigated the elastoplastic dynamic time-history analysis of damaged steel frame structures under seismic actions. Finite element models were constructed using OpenSees software, and appropriate seismic records were selected for analysis. Finally, the seismic performance of structures with different parameters was simulated and computed. The main conclusions are as follows:

1. With an increase in the number of storeys, the maximum top displacement of the structure also increases, indicating that the sensitivity and vulnerability of the structure to seismic actions increase with the number of storeys. Particularly, the increase in top displacement is more significant when transitioning from six to nine storeys compared to the transition from three to six storeys. This suggests that taller structures experience faster degradation in performance and are more sensitive to seismic responses. Additionally, an increase in the number of spans leads to a gradual reduction in top displacement, indicating that an increased number of spans improves the structural deformation capacity.

2. The increase in the maximum section damage index (D) does indeed lead to an increase in the maximum top displacement, and this increase exhibits nonlinear characteristics in different damage index ranges. Specifically, when the damage index increases from 0.4652 to 0.6992, there is a notable increase in displacement. However, the rate of increase in displacement decreases when the damage index increases from 0.6992 to 0.8755. This reflects the varying response characteristics of the structure at different damage stages. Even as the damage index continues to increase, the contribution increment to top displacement decreases, especially when the structure experiences significant damage.

References

[1] ATC-63, Quantification of building seismic performance factors, ATC-63 Project Report, FEMA P695/April 2008.

[2] IBC, (2006). International Building Code[S]. International Code Council, 2006, USA.

[3] Wang Jingzhe, Zhu Xi. Acceleration sensitive area of response spectrum under near-field seismic velocity pulse [J]. China Railway Science, 2003, 24(6): 27-30.

[4] WANG Dongsheng, Feng Qimin, Zhai Tong. Seismic performance of reinforced concrete piers under ground motion near faults [J]. Earthquake Engineering and Engineering Vibration, 2003, 23(1): 95-102.